

SUPPORTING INFORMATION

Title: A Triarylated 1,2,3-Triazol-5-ylidene Ligand with a Redox-Active Ferrocenyl Substituent for Rhodium(I)-Catalyzed Hydroformylation of 1-Octene

Author(s): Danielle Aucamp, Tim Witteler, Fabian Dielmann, Shepherd Siangwata, David C. Liles, Gregory S. Smith, Daniela I. Bezuidenhout*

Table of Content

I.	General considerations.....	S2
II.	Synthesis and characterization of ligand precursors A – C	S3
III.	NMR spectra and atom numbering schemes of A – C and free MIC A'	S6
IV.	NMR spectra and atom numbering schemes of complexes 1–7	S11
V.	¹⁹ F NMR spectrum of A_{ox}	S18
VI.	Cyclic voltammograms of A, 1 and 4	S19
VII.	IR data of 4 and 4_{ox}	S21
VIII.	Optimization of hydroformylation catalytic reaction conditions for 1	S22
IX.	References	S23

I. General considerations

Characterisation Techniques

Nuclear magnetic resonance (NMR) spectra were obtained using either a Bruker AVANCE-III-300 operating at 300.13 MHz for ^1H , 75.47 MHz for ^{13}C , 121.49 MHz for ^{31}P and 282.40 MHz for ^{19}F ; or AVANCE-III-400 operating at 400.21 MHz for ^1H , 100.64 MHz for ^{13}C , 162.01 MHz for ^{31}P and 376.57 MHz for ^{19}F . ^1H Chemical shifts are reported as δ (ppm) values downfield from Me_4Si and chemical shifts were referenced to residual non-deuterated solvents peaks (CD_2Cl_2 , 5.32 ppm; CDCl_3 , 7.26 ppm; C_6D_6 , 7.16 ppm; CD_3CN , 1.94 ppm). $^{13}\text{C}\{^1\text{H}\}$ chemical shifts are also reported as δ (ppm) values downfield from Me_4Si and chemical shifts were referenced to residual non-deuterated solvents peaks (CD_2Cl_2 , 54.0 ppm; CDCl_3 , 77.16 ppm; C_6D_6 , 128.06 ppm; CD_3CN , 118.26 ppm). The chemical shifts are given in ppm and the proton coupling constants (J) are given in Hz. The spectral coupling patterns are designated as follows: s - singlet; d - doublet; t - triplet; q - quartet; sept-septet; m - multiplet; br - broad signal. The assignment of the NMR for each complex follows the numbering scheme individually assigned for each compound illustrated on the respective NMR spectra below. An asterisk (*) denotes solvent contaminant in the NMR spectra. Chemical shift assignment in the ^1H NMR spectra is based on first-order analysis and when required were confirmed by two-dimensional (2D) (^1H - ^1H) homonuclear chemical shift correlation (COSY) experiments. The ^{13}C shifts were obtained from proton-decoupled ^{13}C NMR spectra. Where necessary, the multiplicities of the ^{13}C signals were deduced from proton-decoupled DEPT-135 spectra. The resonances of the proton-bearing carbon atoms were correlated with specific proton resonances using 2D (^{13}C - ^1H) heteronuclear single-quantum coherence (HSQC) experiments. Standard Bruker pulse programs were used in the experiments.

Single crystal X-ray diffraction data for **B** and **C** were collected on a Bruker Apex II-CCD detector using Mo-K_α radiation ($\lambda = 0.71073 \text{ \AA}$). Crystals were selected under oil, mounted on nylon loops then immediately placed in a cold stream of N_2 at 150 K. Structures were solved and refined using Olex2 and SHELXTL.¹

Solution IR spectra ($\nu(\text{CO})$) were recorded on a Bruker ALPHA FT-IR spectrophotometer with a NaCl cell, using CH_2Cl_2 as solvent. The range of absorption measured was from 4000-600 cm^{-1} .

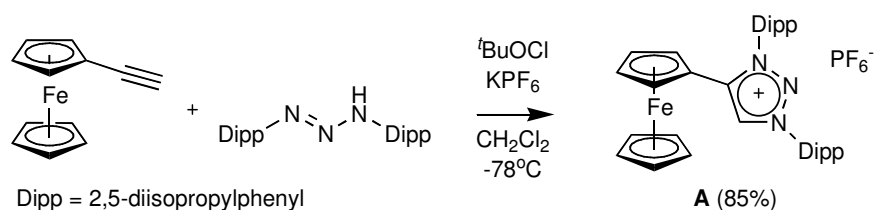
Mass spectral analyses were performed on a Waters Synapt G2 HDMS by direct infusion at 5 $\mu\text{L}/\text{min}$ with positive electron spray as the ionization technique. The m/z values were measured in the range of

400-1500 with acetonitrile as solvent. Prior to analysis, a 5 mM sodium formate solution was used to calibrate the instrument in resolution mode.

Elemental analyses were carried out using a Thermo Flash 1112 Series CHNS-O Analyzer, and melting points were measured with a Stuart SMP10 melting point apparatus.

II. Synthesis and characterization of ligand precursors A – C

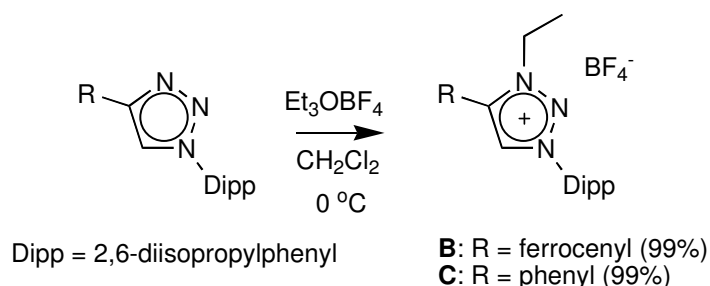
Synthesis of 1,3-bis(2,6-diisopropylphenyl)-4-ferrocenyl-1H-1,2,3-triazolium hexafluorophosphate(V) (**A**).



Scheme S1. Synthesis of triazolium salt **A**

An adapted procedure of the previously reported method for diarylated triazolium salt synthesis was followed.² Ethynylferrocene (1.00 g, 4.76 mmol), 2 equivalents of triazene (3.48 g, 9.52 mmol) and excess KPF_6 (2.00 g, 10.8 mmol) were added to a purged Schlenk vessel and dissolved in anhydrous dichloromethane (DCM). The solution was cooled to $-78\text{ }^\circ\text{C}$ and 2 equivalents of *tert*-butylhypochlorite (1.08 mL, 9.52 mmol) were added dropwise. The solution was kept cold for at least 5 hours and then left to warm up to room temperature overnight. After filtration, the filtrate was concentrated under reduced pressure and the solid was triturated with hexane and diethyl ether, affording **A** as an orange powder. Yield: 2.9 g (85%). M.p: $215\text{--}220\text{ }^\circ\text{C}$ (decomp). ^1H NMR (300 MHz, CD_3CN) δ 9.06 (s, 1H, trz-H, **H-1**), 7.77 (t, $J = 7.9$ Hz, 2H, dipp-H, **H-2**), 7.56 (dd, $J = 7.7, 6.0$ Hz, 4H, dipp-H, **H-3**), 4.56 (m, 2H, Fc-H, **H-4**), 4.35 (m, 2H, Fc-H, **H-5**), 4.25 (s, 5H, Fc-H, **H-6**), 2.42 (dd, $J = 13.6, 6.8$ Hz, 2H, dipp(iso)-CH, **H-7**), 2.34 (dd, $J = 13.1, 6.4$ Hz, 2H, dipp(iso)-CH, **H-7**), 1.36 (d, $J = 6.8$ Hz, 6H, dipp(iso)-CH₃, **H-8**), 1.23 (d, $J = 6.8$ Hz, 6H, dipp(iso)-CH₃, **H-8**), 1.18 (d, $J = 6.9$ Hz, 6H, dipp(iso)-CH₃, **H-8**), 1.15 (d, $J = 6.9$ Hz, 6H, dipp(iso)-CH₃, **H-8**). ^{13}C $\{^1\text{H}\}$ NMR (75 MHz, CD_3CN) δ 149.0 (Trz-C_q, **C-1**), 146.5 (dipp-C_q, **C-2**), 146.2 (dipp-C_q, **C-2**), 134.6 (dipp-C_q, **C-3**), 134.4 (dipp-C_q, **C-3**), 131.5 (Trz-CH, **C-4**), 131.3 (dipp-CH, **C-5**), 130.4 (dipp-CH, **C-5**), 126.5 (dipp-CH, **C-6**), 126.1 (dipp-CH, **C-6**), 73.2 (Fc-CH, **C-7**), 71.8 (Fc-CH, **C-8**), 70.4 (Fc-CH, **C-9**), 64.6 (Fc-C_q, **C-10**), 30.2 (dipp(iso)-CH, **C-11**), 25.2 (dipp(iso)-CH₃, **C-12**), 24.5 (dipp(iso)-CH₃, **C-12**), 24.1 (dipp(iso)-CH₃, **C-12**), 22.8 (dipp(iso)-CH₃, **C-12**). ^{31}P $\{^1\text{H}\}$ NMR (121 MHz, CD_3CN) δ -144.61 (sept, $J = 706.3$ Hz, PF_6^-). ^{19}F

$\{^1\text{H}\}$ NMR (282 MHz, CD_3CN) δ -72.95 (d, J = 706.3 Hz, PF_6). Anal. Calcd for $\text{C}_{36}\text{H}_{44}\text{N}_3\text{FePF}_6$: C 56.55, H 5.80, N 5.50. Found: C 56.19, H 5.51, N 5.50. ESI-HRMS (15 V, positive mode, m/z): calcd for $[\text{M}]^+$: 574.2884. Found: 574.2893.



Scheme S2. Synthesis of triazolium salts B and C.

The precursor salts **B** and **C** were synthesized from their corresponding known precursor triazoles.³ To a solution of the appropriate triazole derivative (2.4 mmol) in DCM, a solution of 3 equivalents of triethyloxonium tetrafluoroborate (7.2 mmol, 1.4 g), in *ca.* 10 mL of solvent DCM was added at -30 °C and left to reach room temperature overnight. After evaporation of the solvent, the solid was dissolved in minimum ethyl acetate (2 mL) after which diethyl ether (20 mL) was added and stirred for 1 hour. The precipitate was filtered and dried to yield the corresponding triazolium salt.

1-ethyl-3-(2,6-diisopropylphenyl)-4-ferrocenyl-1*H*-1,2,3-triazolium tetrafluoroborate(III) **B**: Orange powder. Yield: 1.3 mg (99 %). M.p. 194–198 °C (decomp). ^1H NMR (300 MHz, CD_3CN) δ 8.67 (s, 1H, trz-H, **H-1**), 7.72 (t, J = 7.8 Hz, 1H, dipp-H, **H-2**), 7.51 (d, J = 7.8 Hz, 2H, dipp-H, **H-3**), 4.90 (d, J = 1.7 Hz, 2H, Fc-H, **H-4**), 4.70 (m, J = 7.2 Hz, 4H, Fc-H (2H), **H-6** and CH_3CH_2 (2H), **H-5**), 4.30 (s, 5H, Fc-H, **H-7**), 2.30 (m, 2H, dipp(iso)-CH, **H-8**), 1.65 (t, J = 7.2 Hz, 3H, CH_2CH_3 , **H-9**), 1.22 (dd, J = 20.4, 6.8 Hz, 12H, dipp(iso)- CH_3 , **H-10**). ^{13}C $\{^1\text{H}\}$ NMR (75 MHz, CD_3CN) δ 146.5 (dipp- C_q , **C-1**), 145.5 (dipp- C_q , **C-2**), 133.9 (dipp-CH, **C-3**), 131.9 (trz- C_q , **C-4**), 131.1 (trz-CH, **C-5**), 125.8 (dipp-CH, **C-6**), 72.6 (Fc-CH, **C-7**), 71.5 (Fc-CH, **C-8**), 70.6 (Fc-CH, **C-9**), 66.2 (Fc- C_q , **C-10**), 49.3 ($-\text{CH}_3\text{CH}_2$, **C-11**), 29.5 (dipp(iso)-CH, **C-12**), 24.4 (dipp(iso)- CH_3 , **C-13**), 23.9 (dipp(iso)- CH_3 , **C-13**), 13.8 ($-\text{CH}_2\text{CH}_3$, **C-14**). ^{19}F NMR (282 MHz, CD_3CN) δ -151.69 (d, J = 15.0 Hz, BF_4). Anal. Calcd for $\text{C}_{26}\text{H}_{32}\text{N}_3\text{FeBF}_4$: C 58.41, H 6.03, N 7.86. Found: C 58.41, H 5.745, N 7.56. ESI-HRMS (15 V, positive mode, m/z): calcd for $[\text{M}]^+$: 442.1945. Found: 442.1904

1-ethyl-3-(2,6-diisopropylphenyl)-4-phenyl-1*H*-1,2,3-triazolium tetrafluoroborate(III) **C**: White crystalline powder. Yield: 1.0 g, 99%. M.p. 94–98 °C. ^1H NMR (300 MHz, CD_3CN) δ 8.66 (s, 1H, trz-H, **H-1**), 7.75 (m,

5H, Ph-CH, **H-3** + m, 1H, dipp-CH, **H-2** at 7.72), 7.52 (d, $J = 7.8$ Hz, 2H, dipp-CH, **H-4**), 4.68 (q, $J = 7.2$ Hz, 2H, -CH₂CH₃, **H-5**), 2.40 (m, 2H, dipp-(iso)-CH, **H-6**), 1.62 (t, $J = 7.2$ Hz, 3H, -CH₂CH₃, **H-7**), 1.21 (dd, $J = 15.0, 6.8$ Hz, 12H, dipp-(iso)-CH₃, **H-8**). ¹³C {¹H} NMR (75 MHz, CD₃CN) δ 146.6 (dipp-C_q, **C-1**), 144.7 (dipp-C_q, **C-2**), 133.9 (dipp-CH, **C-3**), 132.9 (Ph-CH, **C-4**), 132.0 (Ph-CH, **C-4**) 131.9 (trz-C_q, **C-5**) 130.8 (trz-CH, **C-6**), 130.5 (Ph-CH, **C-4**), 125.8 (dipp-CH, **C-7**), 123.1 (Ph-C_q, **C-8**), 49.3 (-CH₂CH₃, **C-9**), 29.4 (dipp-(iso)-CH, **C-10**), 24.7 (dipp-(iso)-CH₃, **C-11**), 23.7 (dipp-(iso)-CH₃, **C-11**), 13.9 (-CH₂CH₃, **C-12**). ¹⁹F NMR (282 MHz, CD₃CN) δ -151.82 (d, $J = 15.0$ Hz). Anal. Calcd for C₂₂H₂₈N₃BF₄: C 60.40 H 6.45 N 9.60. Found: C 60.61 H 6.20 N 9.46. ESI-HRMS (15 V, positive mode, m/z): calcd for [M]⁺: 334.2283. Found: 334.2247.

Single crystal X-ray structures of compounds **B** and **C**

Suitable crystals of **B** and **C** for X-ray diffraction were obtained from a layered concentrated DCM solution and toluene (1:9).

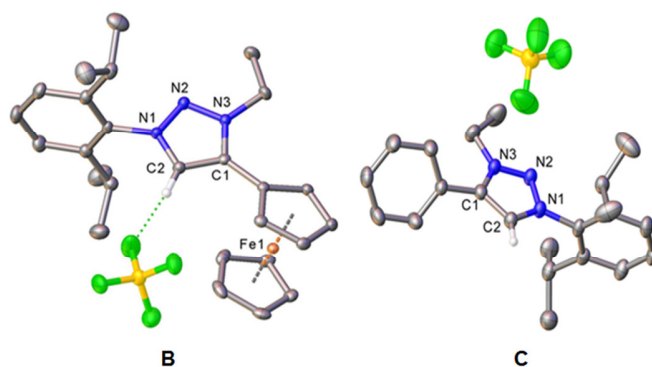


Figure S1. Molecular structures of triazolium salts **B** and **C**, showing 50% probability ellipsoids and partial atom-numbering scheme. Hydrogens (except for trz-H) are omitted for clarity.

Crystal data for compound **B**

C₂₆H₃₂BF₄FeN₃ (M = 529.20 g/mol): monoclinic, space group C2/c, a = 29.3111(19) Å, b = 9.0993(6) Å, c = 18.6543(12) Å, $\alpha = 90^\circ$, $\beta = 90.198(3)^\circ$, $\gamma = 90^\circ$, V = 4975.3(6) Å³, Z = 8, T = 150 K, D_{calc} = 1.413 g/cm³, $\mu(\text{MoK}\alpha) = 0.656$ mm⁻¹, 86054 reflections measured ($4.368^\circ \leq 2\theta \leq 52.91^\circ$), 5134 unique [$R_{int} = 0.0323$, $R_{sigma} = 0.0133$] which were used in all calculations. The final R_1 was 0.0293 ($I > 2\sigma(I)$) and wR_2 was 0.0705 (all data).

Crystal data for compound **C**

$C_{22}H_{28}BF_4N_3$ ($M = 421.28$ g/mol): monoclinic, space group $CP2_1/c$, $a = 8.2036(7)$ Å, $b = 12.5525(11)$ Å, $c = 21.5301(17)$ Å, $\alpha = 90^\circ$, $\beta = 92.659(4)^\circ$, $\gamma = 90^\circ$, $V = 2214.7(3)$ Å³, $Z = 4$, $T = 150$ K, $D_{calc} = 1.263$ g/cm³, $\mu(CuK\alpha) = 0.822$ mm⁻¹, 75653 reflections measured ($4.368^\circ \leq 2\theta \leq 52.91^\circ$), 4529 unique [$R_{int} = 0.0596$, $R_{sigma} = 0.0255$] which were used in all calculations. The final R_1 was 0.0607 ($I > 2\sigma(I)$) and wR_2 was 0.1544 (all data).

III. NMR spectra and atom numbering schemes of **A – C** and free MIC **A'**

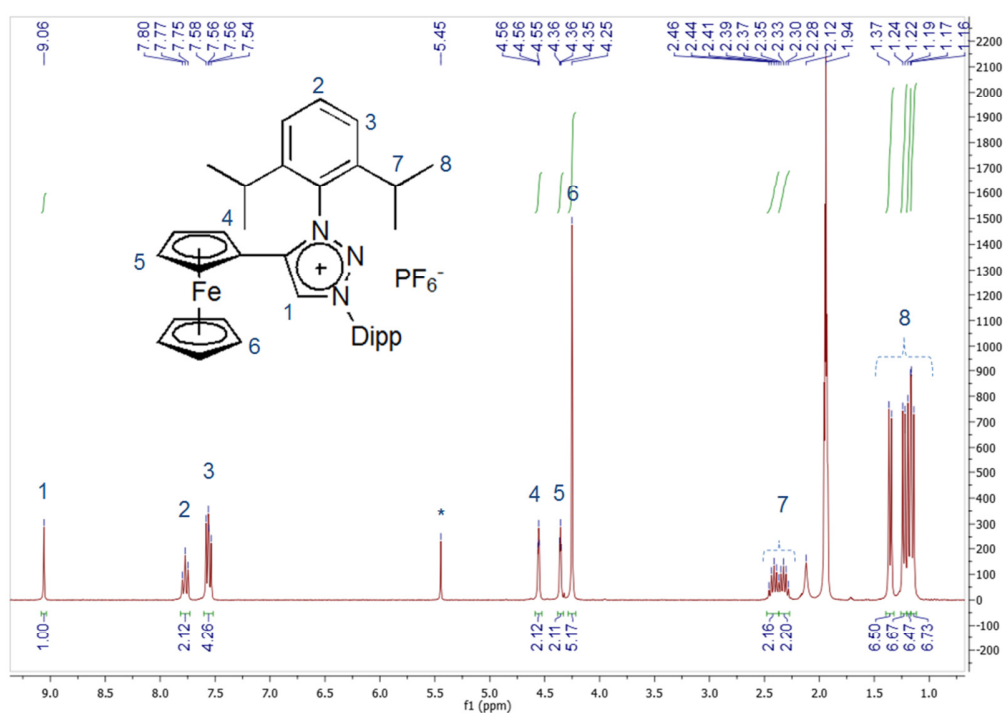


Figure S2. The ¹H NMR spectrum of **A** in solvent CD₃CN.

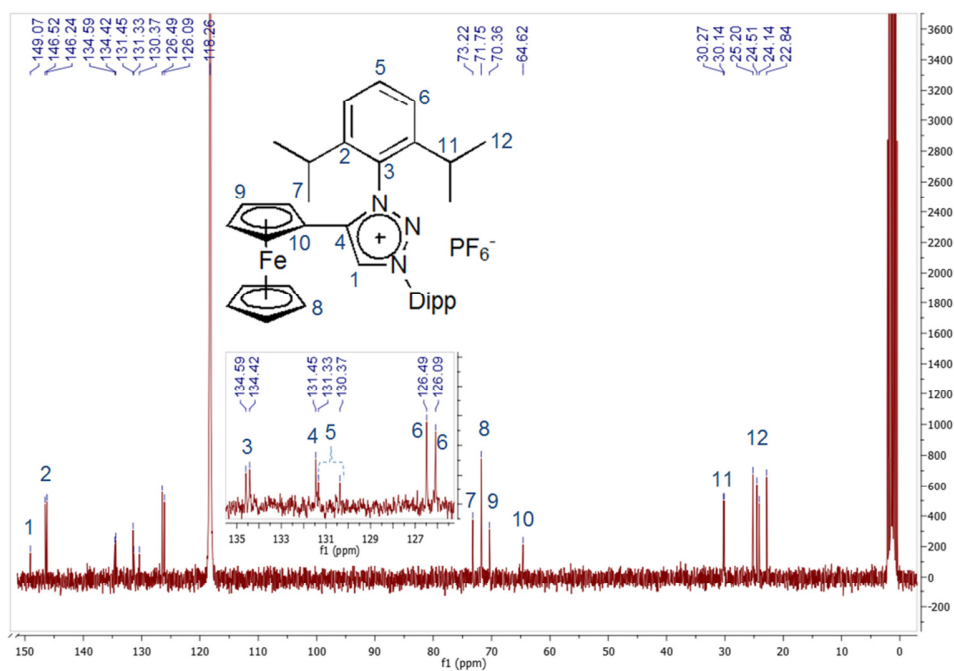


Figure S3. The $^{13}\text{C}\{^1\text{H}\}$ NMR spectrum of **A** in solvent CD_3CN .

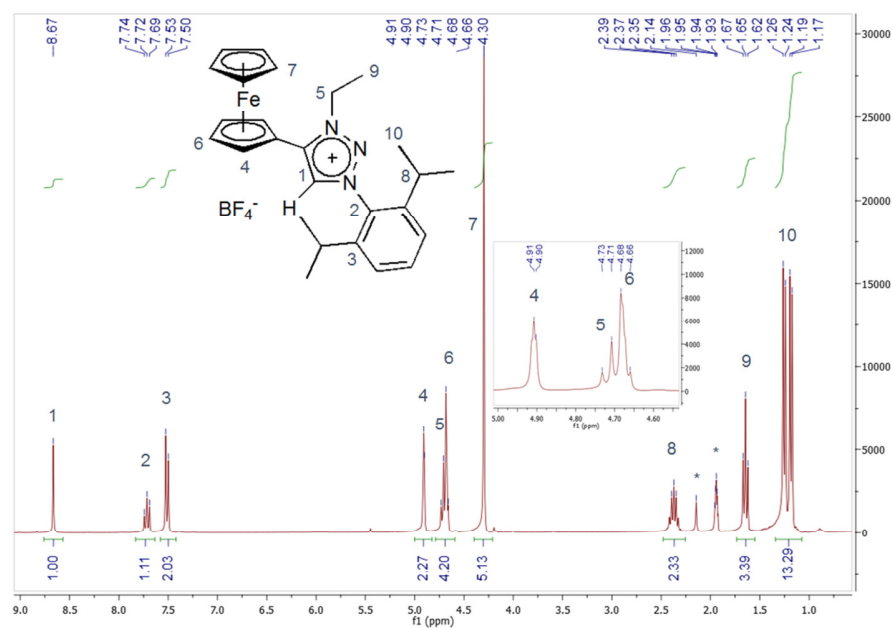


Figure S4. The ^1H NMR spectrum of **B** in solvent CD_3CN .

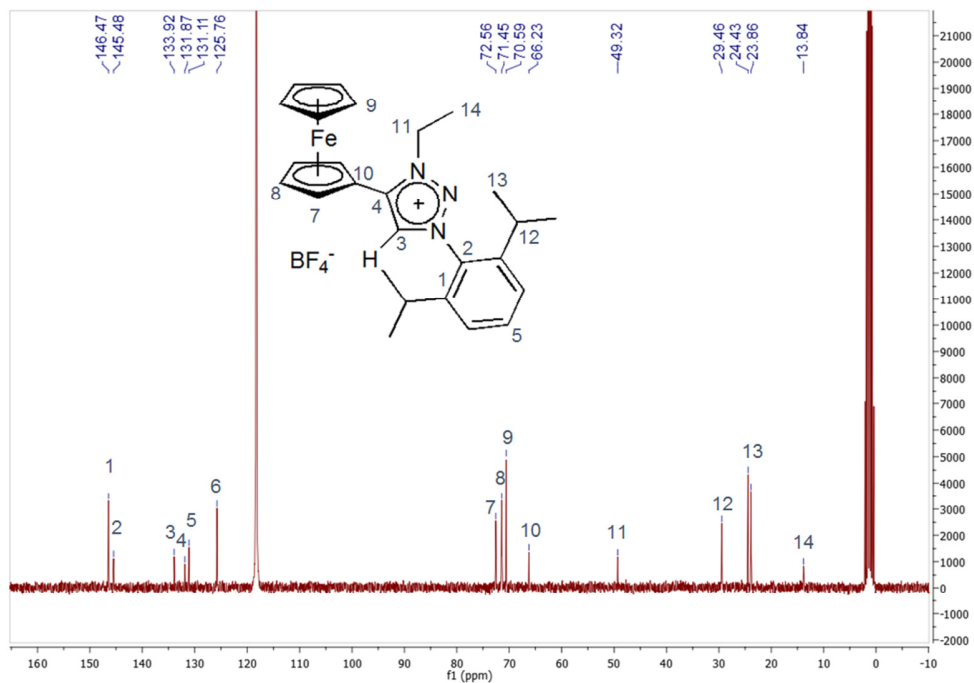


Figure S5. The ^{13}C $\{^1\text{H}\}$ NMR spectrum of **B** in solvent CD_3CN .

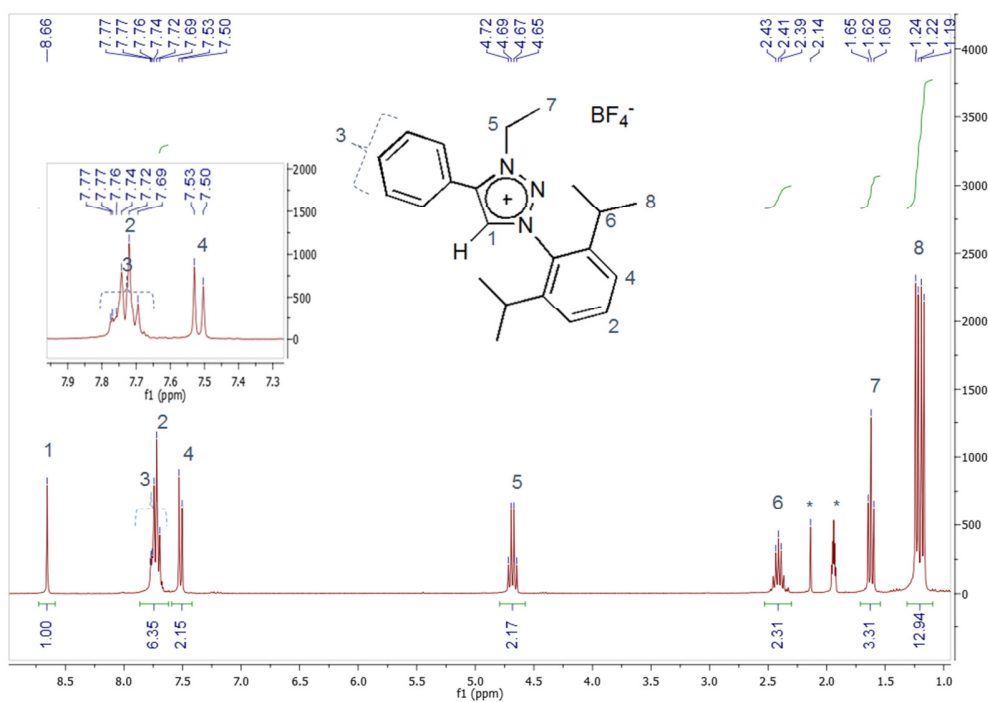


Figure S6. The ^1H NMR spectrum of **C** in solvent CD_3CN .

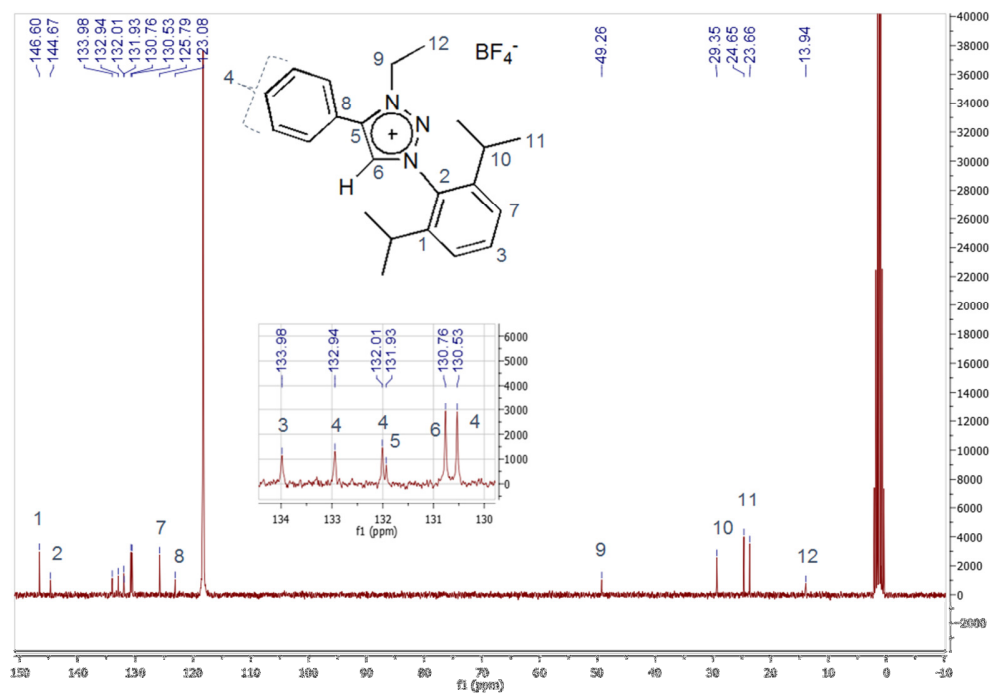


Figure S7. The ^{13}C $\{^1\text{H}\}$ NMR spectrum of **C** in solvent CD_3CN .

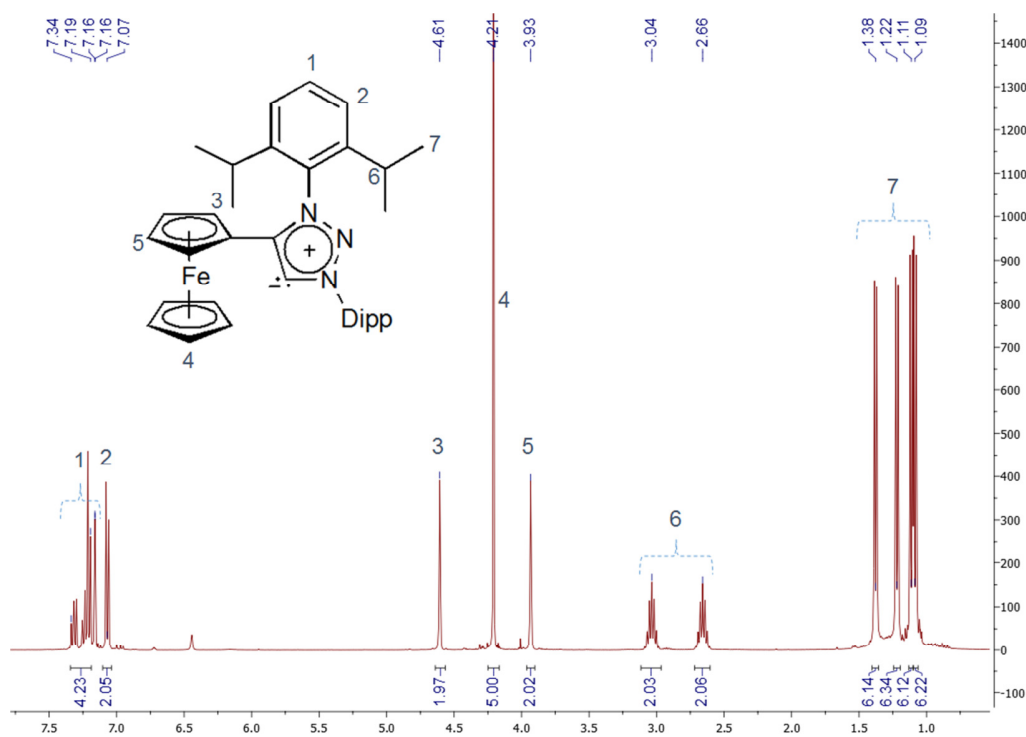


Figure S8. The ^1H NMR spectrum of the free carbene **A'** in solvent C_6D_6 .

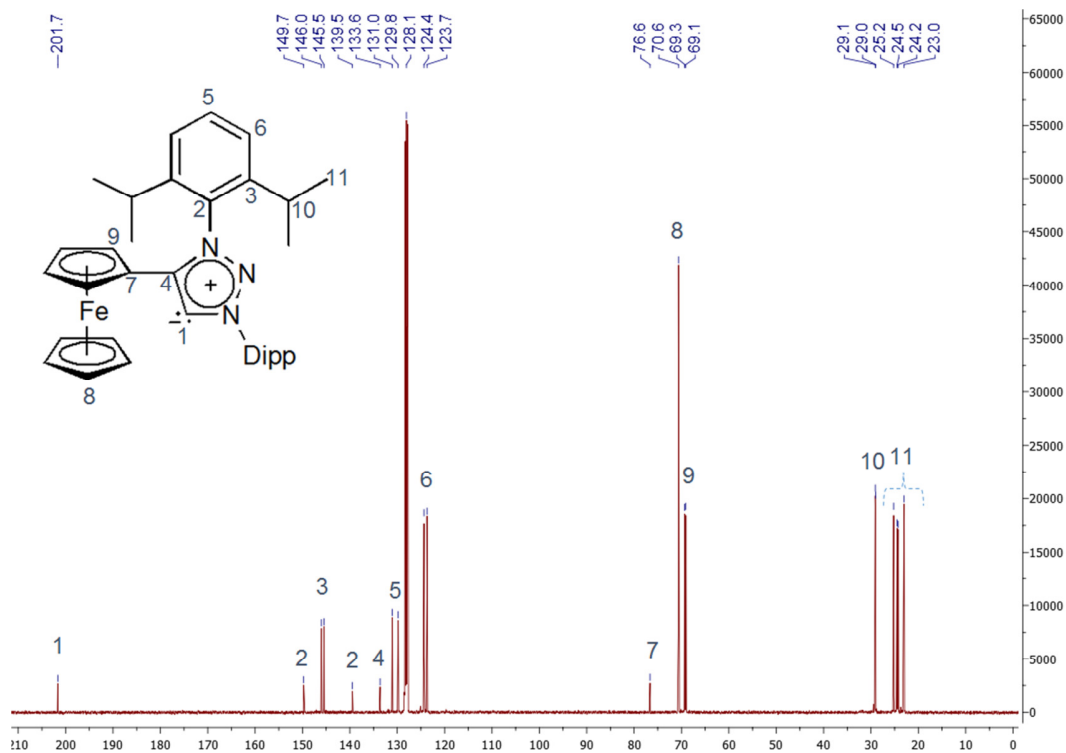


Figure S9. The $^{13}\text{C} \{^1\text{H}\}$ NMR spectrum of the free carbene **A'** in solvent C_6D_6 .

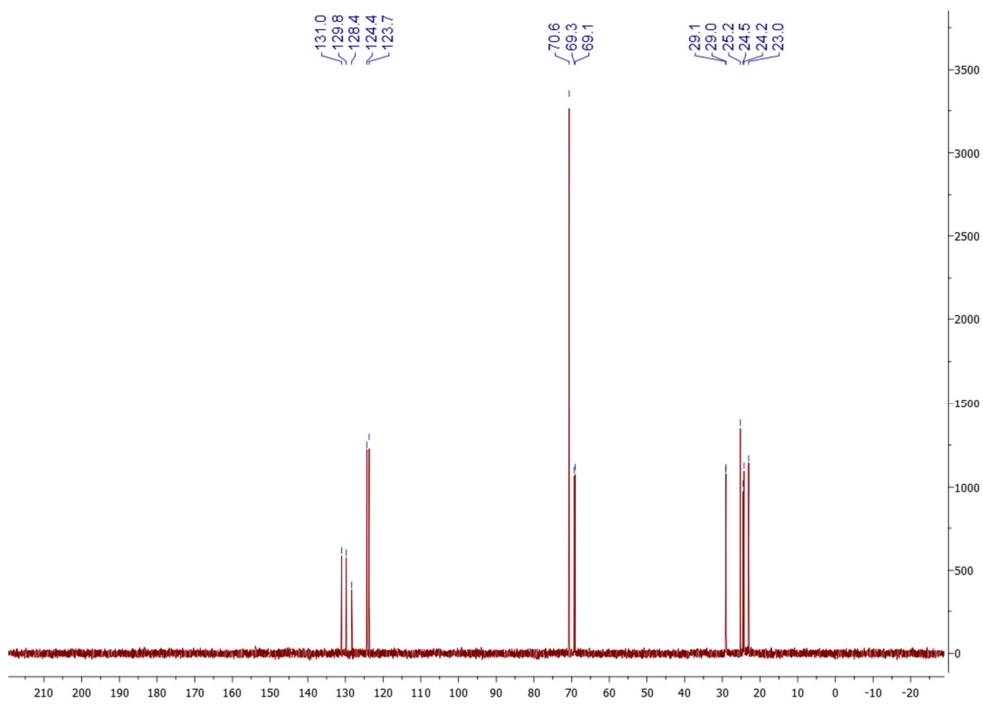


Figure S10. The ^{13}C DEPT135 NMR spectrum of the free carbene **A'** in solvent C_6D_6 .

IV. NMR spectra and atom numbering schemes of complexes 1–7

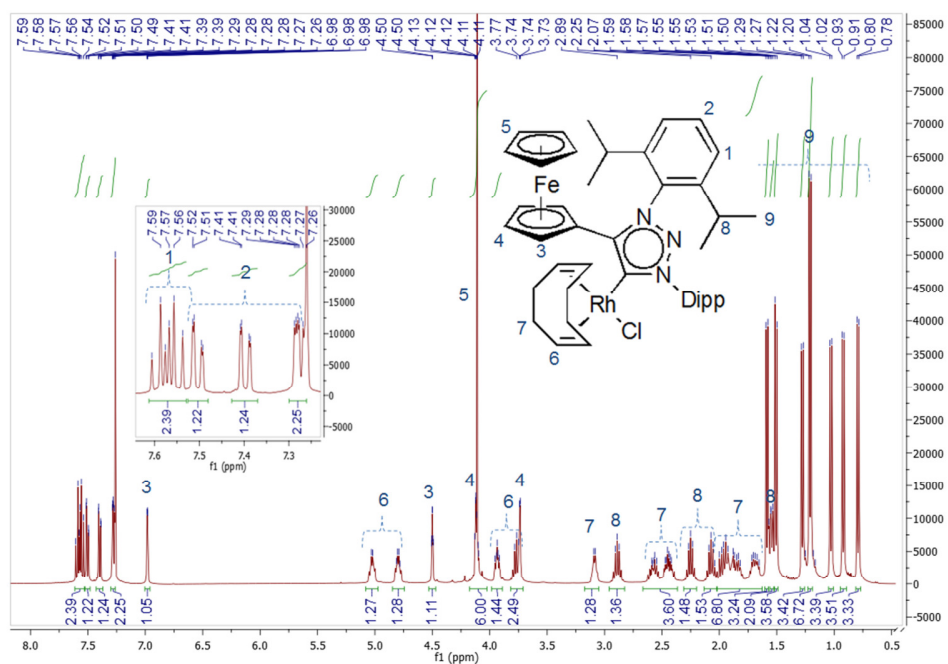


Figure S11. The ^1H NMR spectrum of **1** in solvent CDCl_3 .

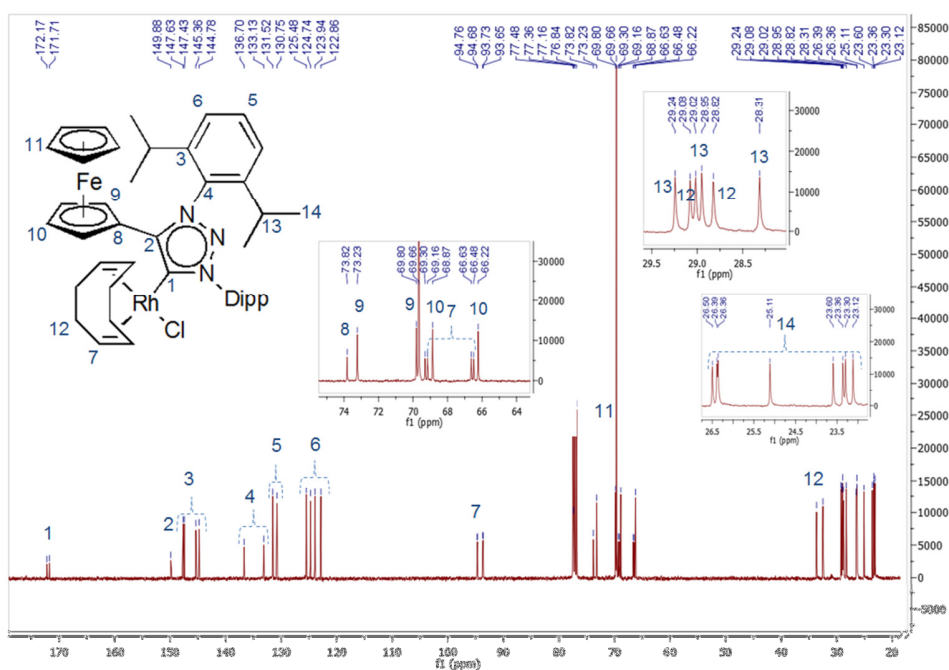


Figure S12. The $^{13}\text{C}\{^1\text{H}\}$ NMR spectrum of **1** in solvent CDCl_3 .

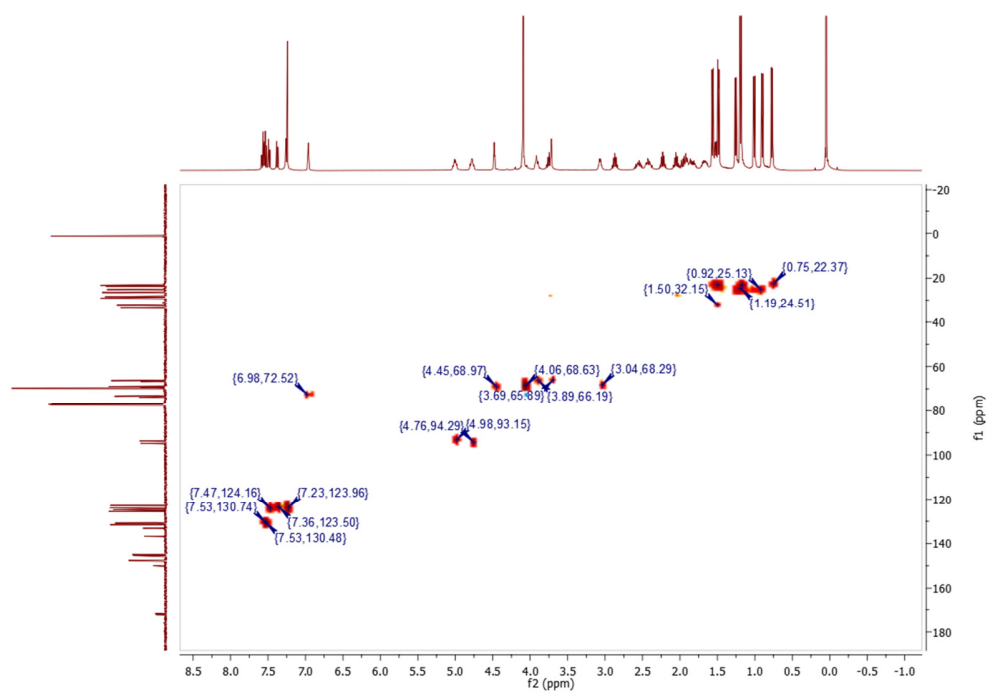


Figure S13. The HSQC (2D-NMR) spectrum of **1** in solvent CDCl_3 .

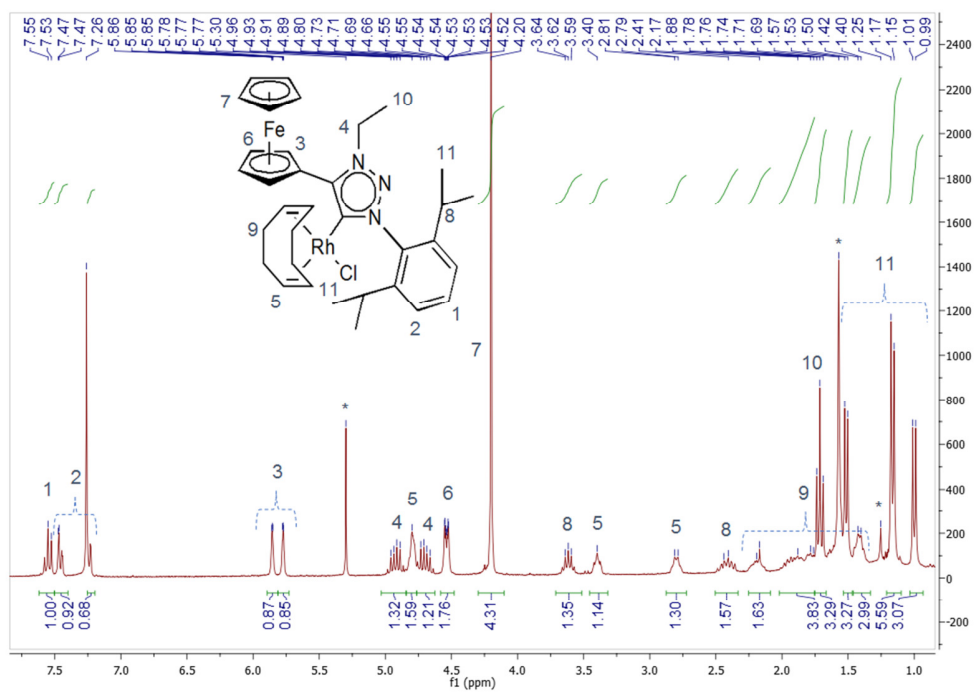


Figure S14. The ^1H NMR spectrum of **2** in solvent CDCl_3 .

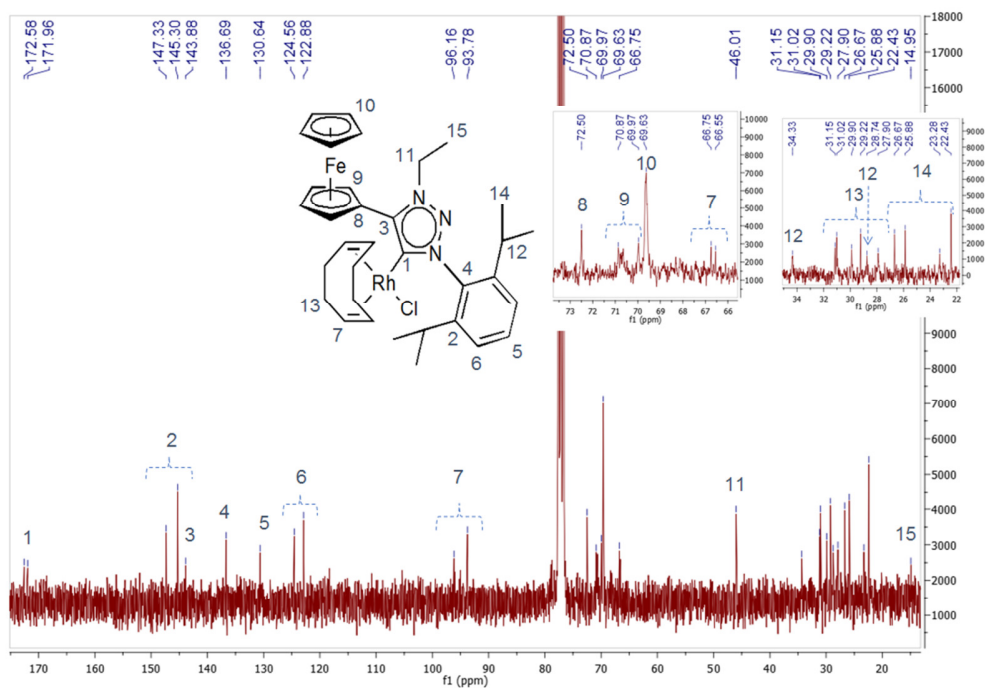


Figure S15. The ^{13}C $\{^1\text{H}\}$ NMR spectrum of **2** in solvent CDCl_3 .

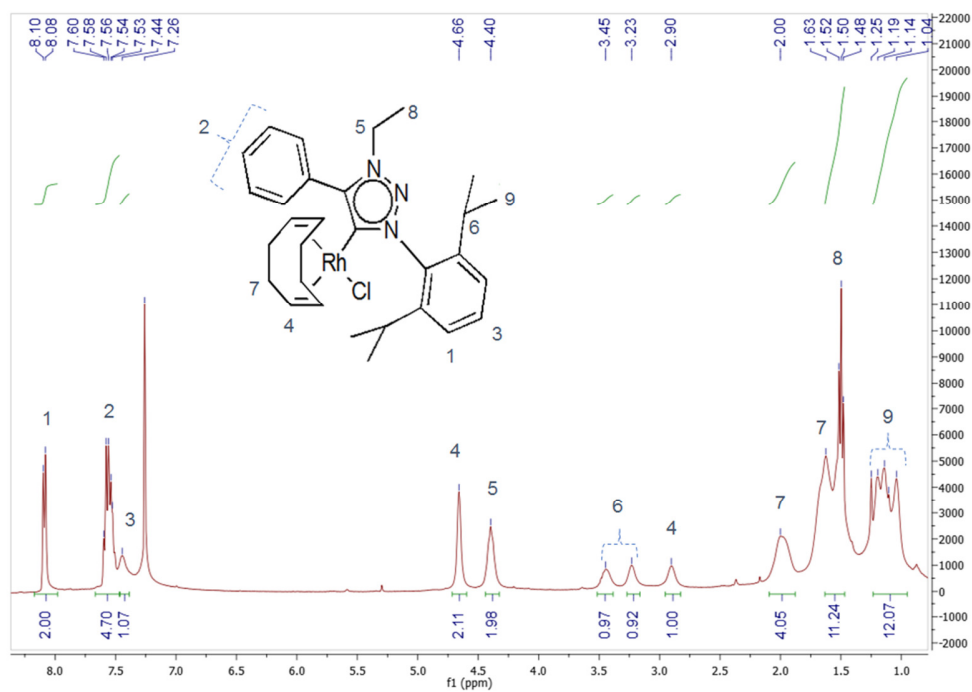


Figure S16. The ^1H NMR spectrum of **3** in solvent CDCl_3 .

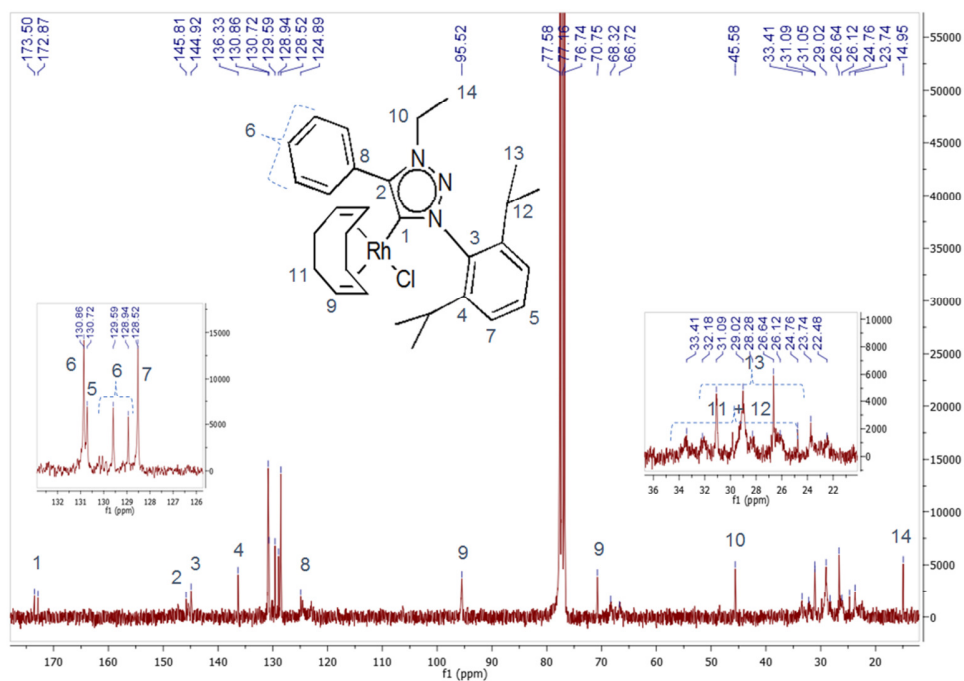


Figure S17. The ^{13}C $\{^1\text{H}\}$ NMR spectrum of **3** in solvent CDCl_3 .

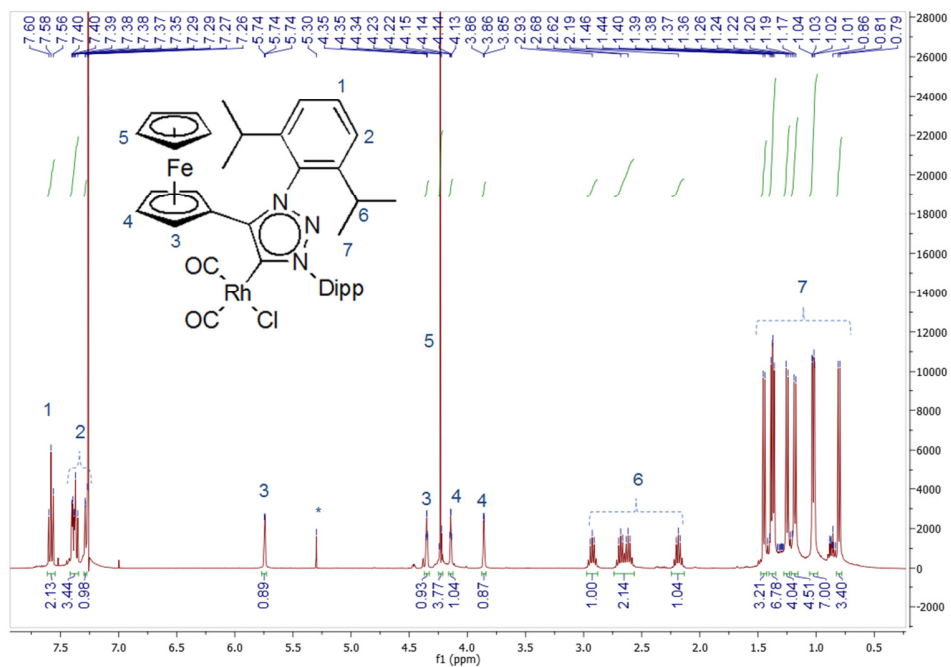


Figure S18. The ^1H NMR spectrum of **4** in solvent CDCl_3 .

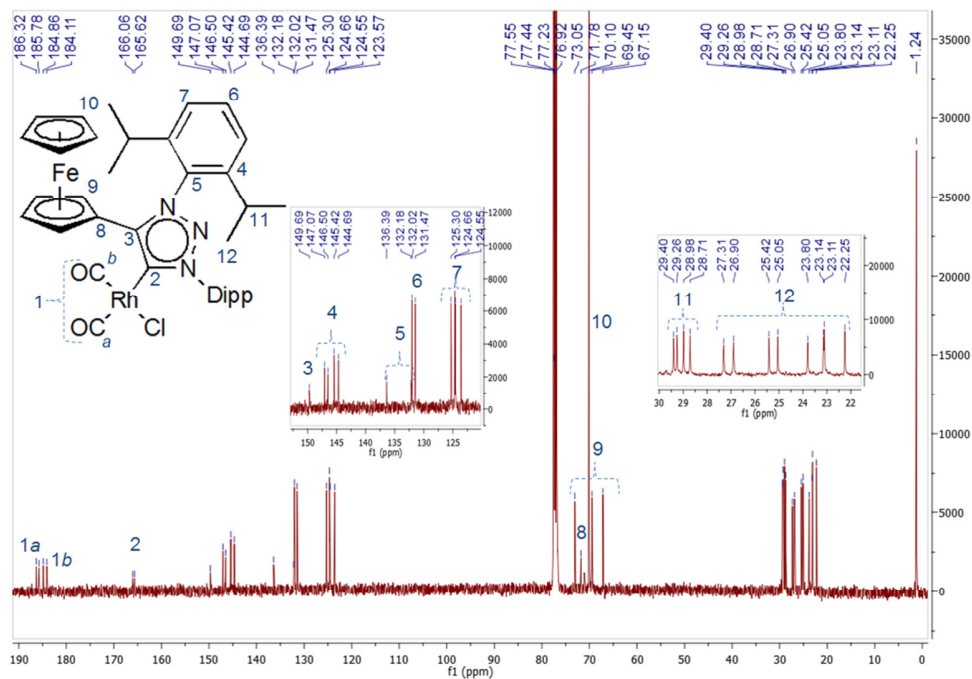


Figure S19. The ^{13}C $\{^1\text{H}\}$ NMR spectrum of **4** in solvent CDCl_3 .

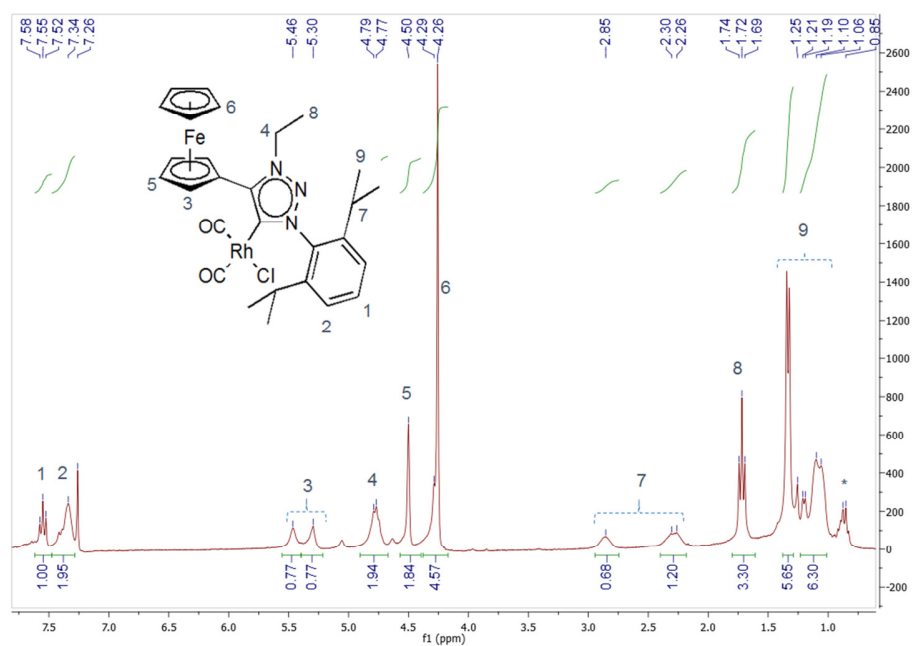


Figure S20. The ^1H NMR spectrum of **5** in solvent CDCl_3 .

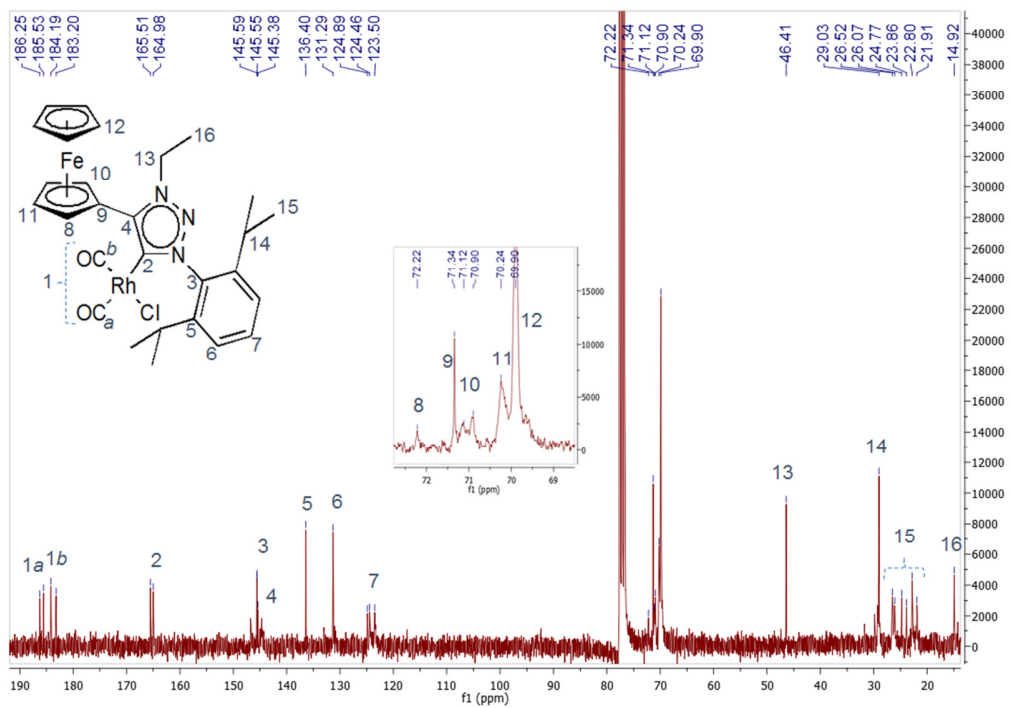


Figure S21. The $^{13}\text{C}\{^1\text{H}\}$ NMR spectrum of **5** in solvent CDCl_3 .

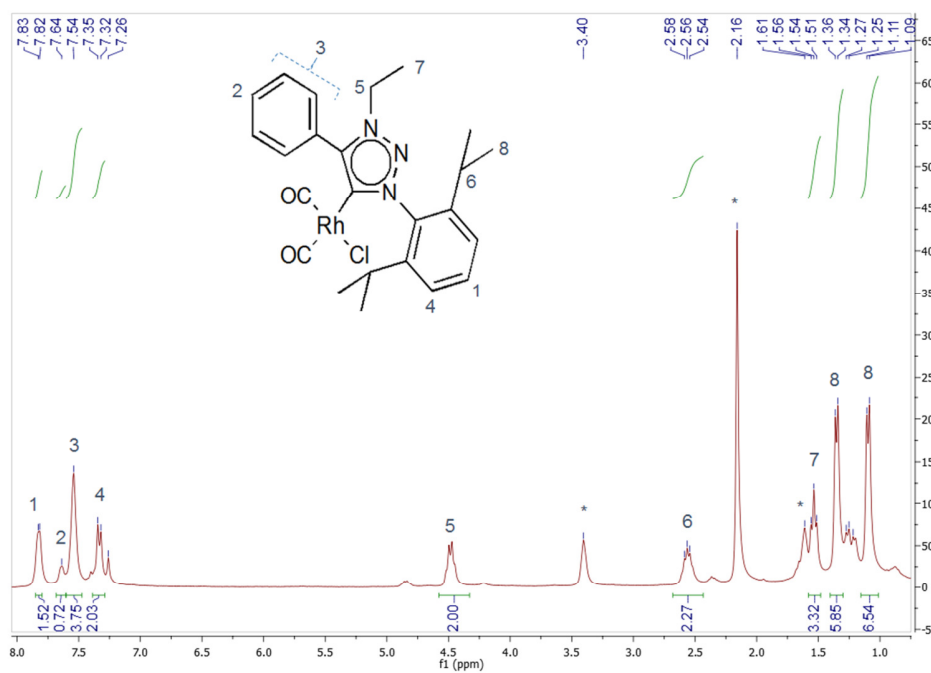


Figure S22. The ^1H NMR spectrum of **6** in solvent CDCl_3 .

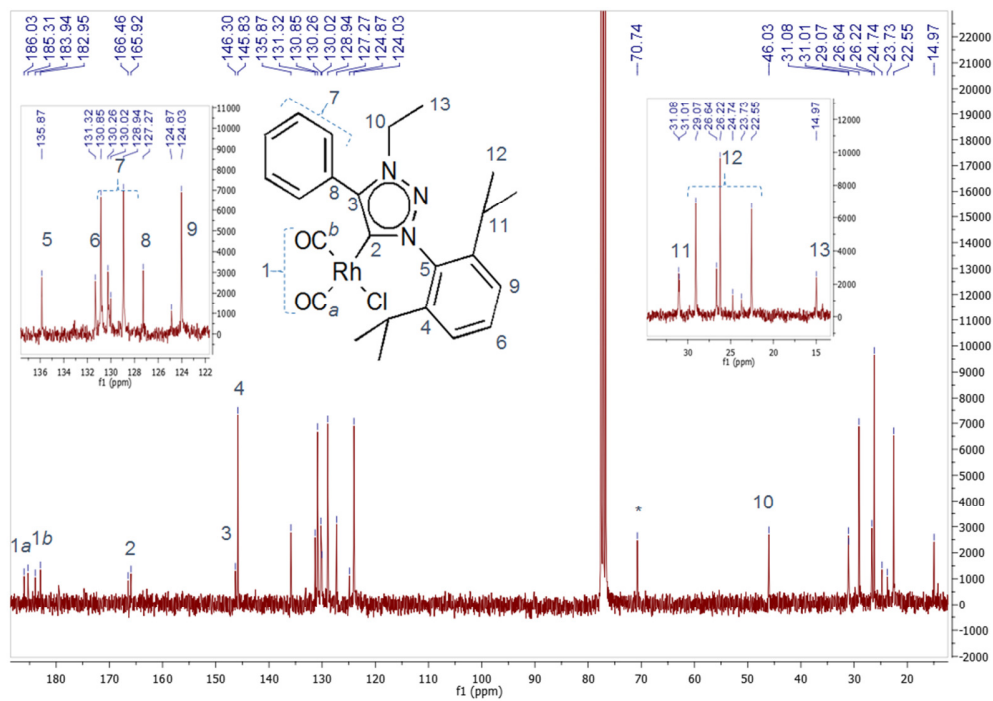


Figure S23. The ^{13}C $\{^1\text{H}\}$ NMR spectrum of **6** in solvent CDCl_3 .

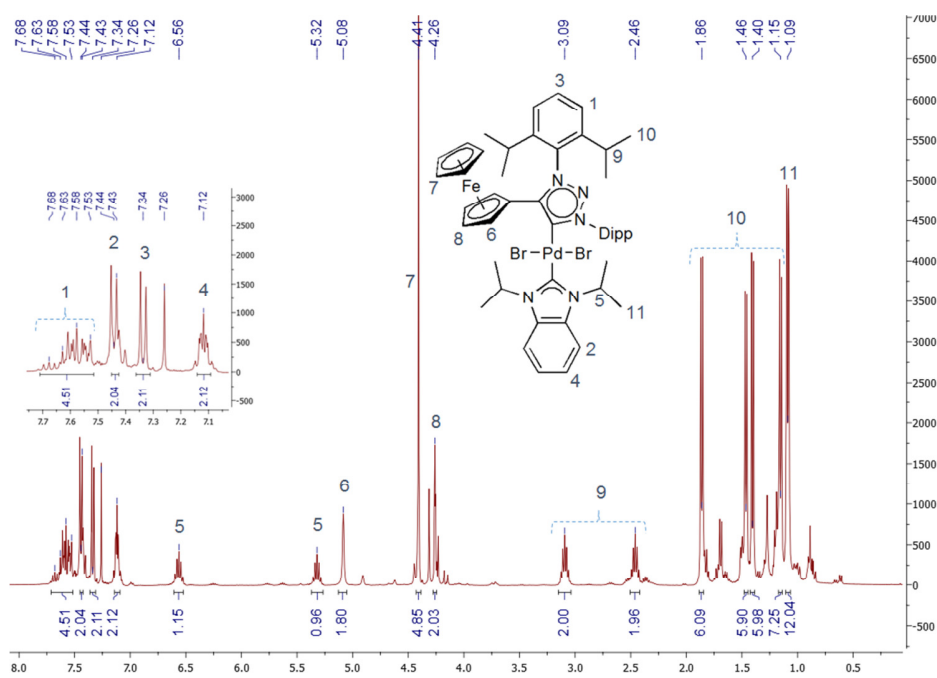


Figure S24. The ^1H NMR spectrum of **7** in solvent CDCl_3 .

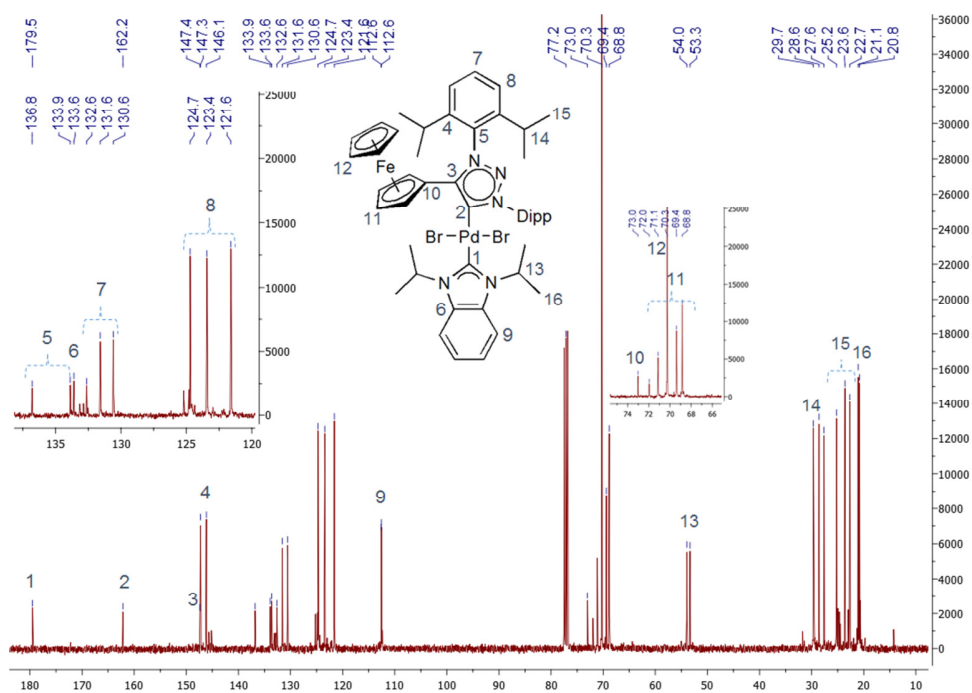


Figure S25. The $^{13}\text{C} \{^1\text{H}\}$ NMR spectrum of complex **7** in solvent CDCl_3 .

V. ^{19}F NMR spectrum of A_{ox}

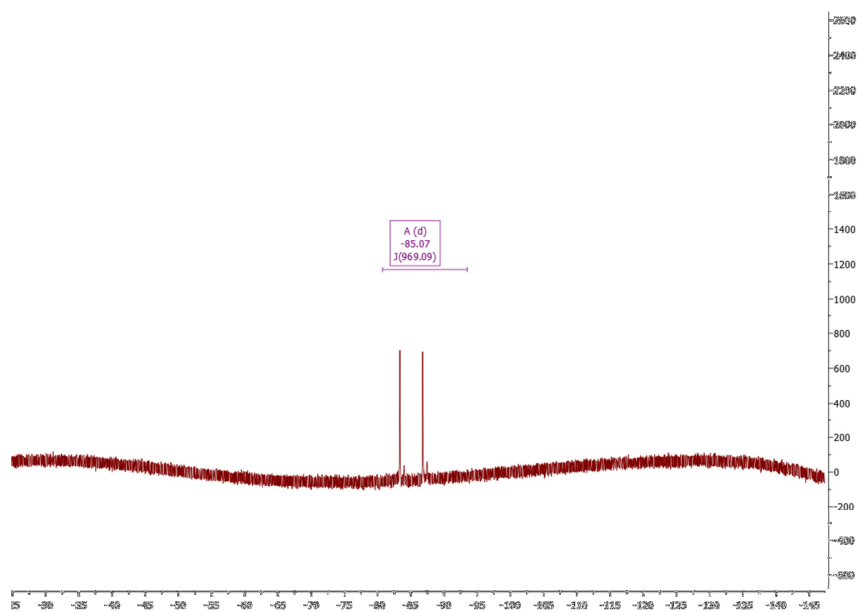


Figure S26. The ^{19}F NMR spectrum of A_{ox} in solvent CD_2Cl_2 .

VI. Cyclic voltammograms of A, 1 and 4

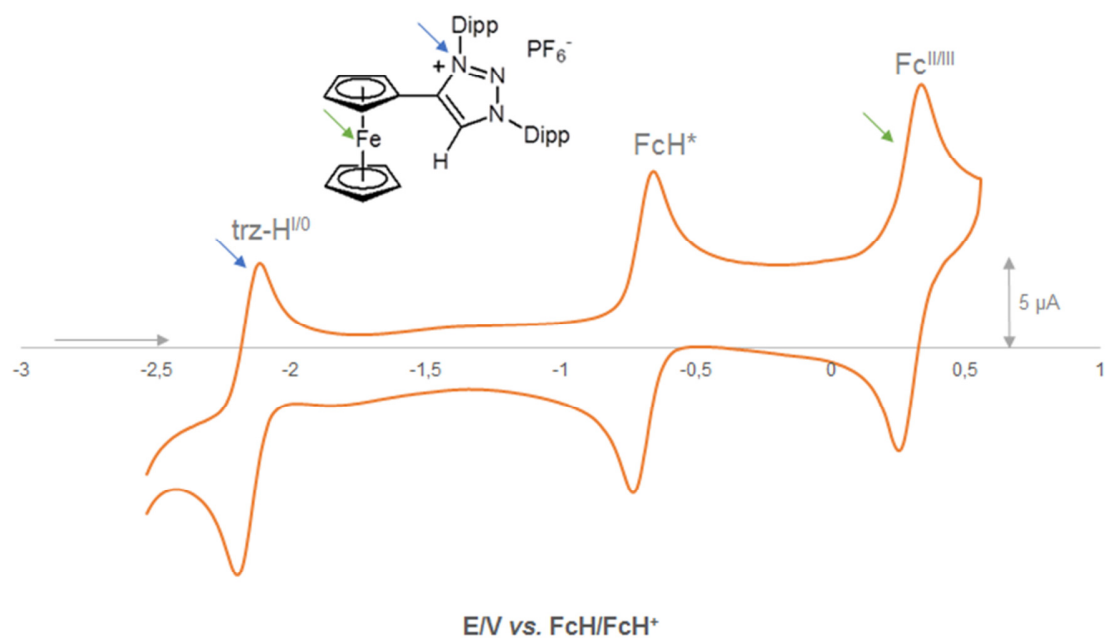


Figure S27. The CV obtained of **A** at a glassy carbon electrode at a scan rate of $0.1 \text{ V} \cdot \text{s}^{-1}$ in CH_2Cl_2 , with decamethylferrocene (FcH⁺) as internal standard.

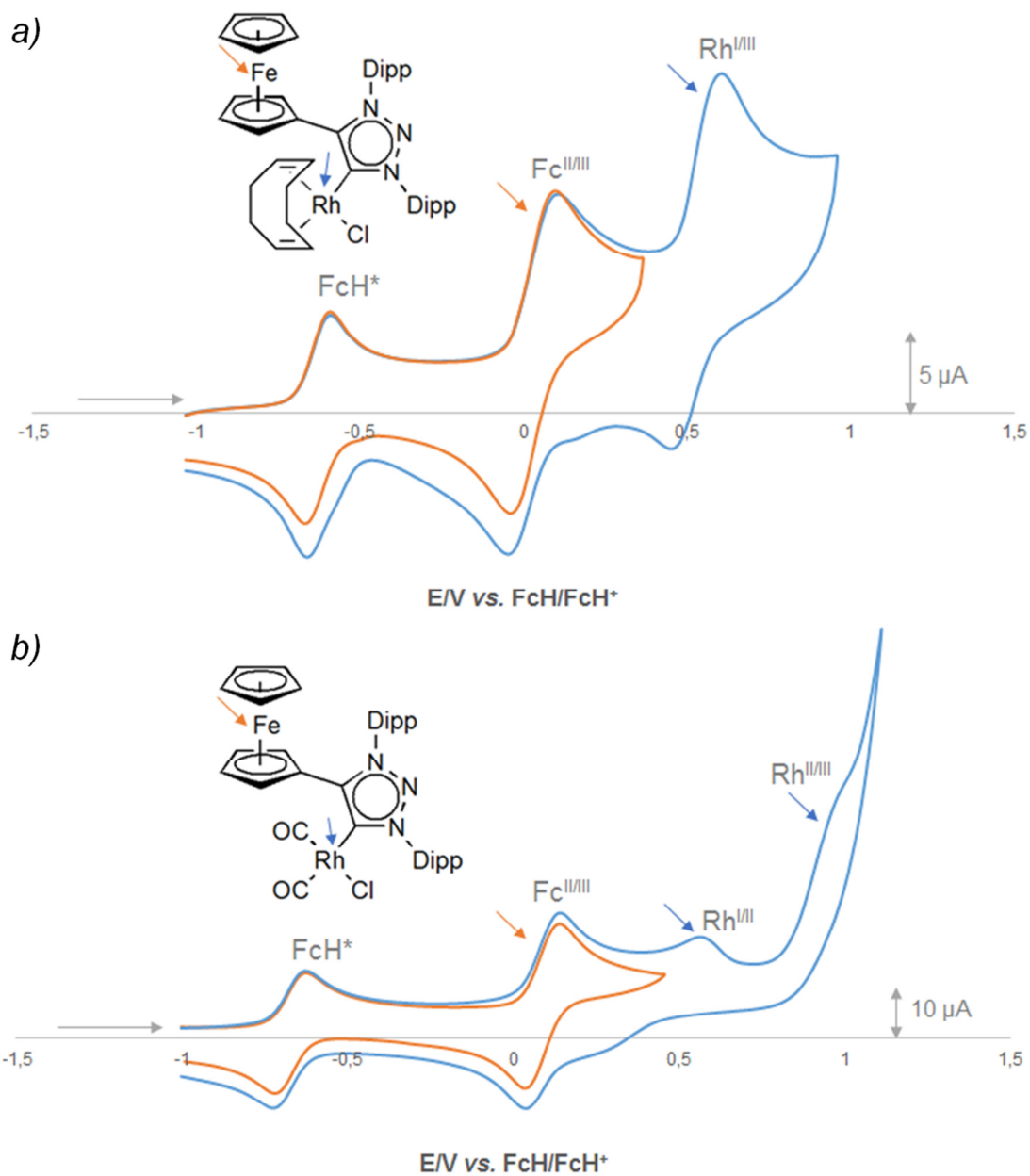


Figure S28. The CVs obtained for (a) **1** and (b) **4** at a glassy carbon electrode at a scan rate of $0.1 \text{ V} \cdot \text{s}^{-1}$ in CH_2Cl_2 , with decamethylferrocene (FcH^*) as internal standard. In both cases, the redox event of the ferrocenyl moiety (after curtailing the scan at 0.5 V), is overlaid in orange.

VII. IR data of **4** and **4_{ox}**

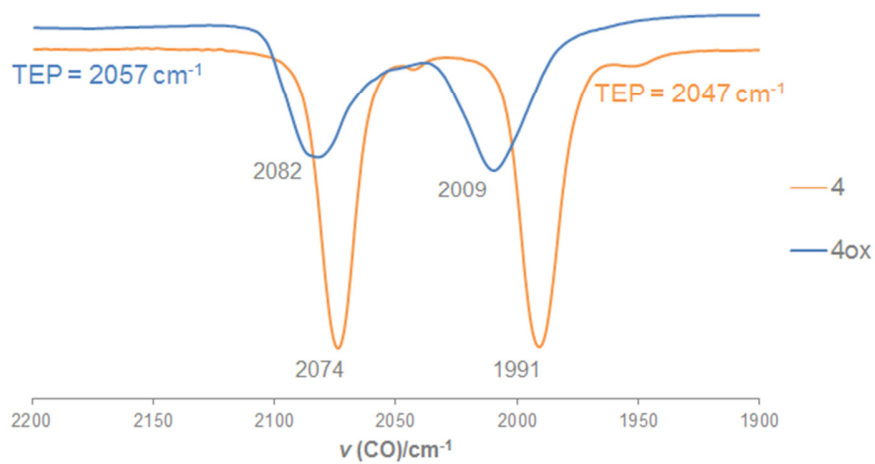


Figure S29. The carbonyl stretching frequencies obtained from IR measurements in solvent DCM of the complexes **4** and **4_{ox}**. The calculated TEP values in cm^{-1} , calculated as $\text{TEP} (\text{cm}^{-1}) [\text{Rh to Ni}] = 0.8001\nu_{\text{CO}}^{\text{av/Rh}} + 420.0 (\text{cm}^{-1})$,⁴ are indicated.

VIII. Optimization of hydroformylation catalytic reaction conditions for 1

Table S1. Optimization results^a of the hydroformylation of 1-octene with catalyst precursor 1.

Entry	Reaction conditions	% conversion	% Aldehydes	% Iso-octene	% Non-anal	% Branched	TOF ^b	TON ^c	n/iso
Variation of syngas pressure and time.									
Temperature = 75 °C; [1]: 1-octene = 1:2500 (0.04 mol %)									
1	40 bar/ 4 hours	69.78 (6.48)	69.76 (4.42)	30.24 (4.42)	69.57 (0.44)	30.43 (0.44)	304.82 (42.40)	1219.30 (169.62)	2.29 (0.05)
	2	40 bar/ 6 hours	85.12 (7.19)	67.48 (9.42)	32.52 (9.42)	68.61 (2.32)	31.39 (2.32)	237.57 (17.72)	1425.41 (106.32)
3	40 bar/ 8 hours	80.76 (8.59)	58.98 (7.91)	41.02 (7.91)	70.26 (2.64)	29.74 (2.64)	148.36 (21.23)	1186.86 (169.80)	2.38 (0.29)
	4	50 bar/ 8 hours	85.93 (15.05)	71.15 (8.33)	28.85 (8.33)	65.88 (0.71)	34.12 (0.71)	188.57 (16.50)	1508.59 (132.04)
Variation of temperature.									
Syngas pressure = 40 bar; time = 8 hr; [1]: 1-octene = 1:1250 (0.08 mol %)									
5	55 °C	56.23 (20.33)	82.38 (16.12)	17.62 (16.12)	59.27 (1.28)	40.73 (1.28)	69.77 (19.74)	558.18 (157.96)	1.46 (0.08)
		6	75 °C	95.83 (2.40)	66.57 (3.39)	33.43 (3.39)	70.59 (3.21)	29.41 (3.21)	99.73 (7.07)
7	95 °C	98.80 (0.40)	69.36 (3.56)	30.64 (3.56)	62.00 (1.76)	38.00 (1.76)	107.06 (5.17)	856.50 (41.39)	1.64 (0.12)
Variation of syngas pressure.									
Temperature = 75 °C; time = 8 hr; [1]: 1-octene = 1:1250 (0.08 mol %)									
8	30 bar	74.77 (18.84)	65.35 (3.09)	34.65 (3.09)	69.82 (0.70)	30.18 (0.70)	75.77 (15.79)	606.17 (126.32)	2.31 (0.08)
		9	50 bar	85.79 (7.56)	77.99 (4.10)	22.01 (4.10)	63.58 (2.81)	36.42 (2.81)	104.78 (13.61)

^aReactions carried out in triplicate, average of three runs given with standard deviation in parentheses.

^bTurnover frequency, calculated as TOF = mol aldehydes/mol cat.h⁻¹

^cTurnover number, calculated as TON = mol aldehydes/mol cat.

IX. References

- [1] a) O. V. Dolomanov, L. J. Bourhis, R. J. Gildea, J. A. K. Howard, H. Puschmann, *J. Appl. Cryst.* **2009**, *42*, 339-341; b) M. C. Burla, R. Caliandro, M. Camalli, B. Carrozzini, G. L. Cascarano, L. De Caro, C. Giacovazzo, G. Polidori, D. Siliqi, R. Spagna, *J. Appl. Cryst.* **2007**, *40*, 609–613; c) G.M. Sheldrick, *Acta Cryst.* **2008**, *A64*, 112–122.
- [2] J. Bouffard, B. K. Keitz, R. Tonner, V. Lavallo, G. Guisado-Barrios, G. Frenking, R. H. Grubbs, G. Bertrand, *Organometallics* **2011**, *30*, 2617–2627.
- [3] a) G. Guisado-Barrios, J. Bouffard, B. Donnadiou, G. Bertrand, *Organometallics*, **2011**, *30*, 6017–6021; b) T. Romero, R.A Orenes. A. Tárraga, P. Molina, *Organometallics*, **2013**, *32*, 5740–5753.
- [4] T. Dröge and F. Glorius, *Angew. Chem. Int. Ed.* **2010**, *49*, 6940–6952.